1016 *Biochemistry* **2011,** *50,* 1016–1022
DOI: 10.1021/bi101895r

BIOCHEMISTRY
including biophysical chemistry & molecular biology
Article

Unusual Heme Binding in the Bacterial Iron Response Regulator Protein: Spectral Characterization of Heme Binding to the Heme Regulatory Motif[†]

Haruto Ishikawa,[‡,¶] Megumi Nakagaki,[‡] Ai Bamba,[‡] Takeshi Uchida,[§] Hiroshi Hori,[∥] Mark R. O'Brian,[⊥] Kazuhiro Iwai,[#] and Koichiro Ishimori*[,‡,§]

[‡]*Department of Molecular Engineering, Graduate School of Engineering, Kyoto University, Kyoto 615-8530, Japan,* [§]*Department of Chemistry, Faculty of Science, Hokkaido University, Sapporo 060-0810, Japan,* [∥]*Department of Mechanical Science and Bioengineering, Graduate School of Engineering Science, Osaka University, Toyonaka 560-8531, Japan,* [⊥]*Department of Biochemistry, State University of New York at Buffalo, Buffalo, New York 14214, United States, and* [#]*Department of Biophysics and Biochemistry, Graduate School of Frontier Biosciences and Graduate School of Medicine, Osaka University, Suita 565-0871, Japan.* [¶]*Current address: Department of Chemistry, Graduate School of Science, Osaka University, Toyonaka 560-0043, Japan.*

Received September 13, 2010; Revised Manuscript Received December 29, 2010

ABSTRACT: We characterized heme binding in the bacterial iron response regulator (Irr) protein, which is a simple heme-regulated protein having a single "heme-regulatory motif", HRM, and plays a key role in the iron homeostasis of a nitrogen-fixing bacterium. The heme titration to wild-type and mutant Irr clearly showed that Irr has two heme binding sites: one of the heme binding sites is in the HRM, where ^{29}Cys is the axial ligand, and the other one, the secondary heme binding site, is located outside of the HRM. The Raman line for the Fe−S stretching mode observed at 333 cm^{-1} unambiguously confirmed heme binding to Cys. The lower frequency of the Fe−S stretching mode corresponds to the weaker Fe−S bond, and the broad Raman line of the Fe−S bond suggests multiple configurations of heme binding. These structural characteristics are definitely different from those of typical hemoproteins. The unusual heme binding in Irr was also evident in the EPR spectra. The characteristic *g*-values of the 5-coordinate Cys-ligated heme and 6-coordinate His/His-ligated heme were observed, while the multiple configurations of heme binding were also confirmed. Such multiple heme configurations are not encountered for typical hemoproteins where the heme functions as the active center. Therefore, we conclude that heme binding to HRM in the heme-regulated protein, Irr, is quite different from that in conventional hemoproteins but characteristic of heme-regulated proteins using heme as the signaling molecule.

Heme is the most common prosthetic group of proteins and serves as an active center for various kinds of proteins essential for respiration, energy generation, chemical processes, and gas sensing *in vivo* (*1*). In addition to these conventional functions of heme, recent studies (*2*−*4*) have revealed that heme functions as a regulatory molecule, not the active centers of proteins, in some "heme-regulated proteins", whose functions are regulated by the binding of heme. Such regulatory functions of heme have been found to play crucial roles in numerous biological processes.

Heme-regulatory motifs (HRMs),[1] which contain a short consensus sequence of Cys and Pro, are found in a wide variety of "heme-regulated" proteins, such as the heme-regulated inhibitor kinase (*5*), heme activator protein (*6*), heme oxygenase (*7*), and circadian factor (*8*). While the deletion of the HRMs in these proteins results in the complete loss of function and the HRMs are supposed to be the essential element for heme regulation in these proteins, the molecular mechanisms of the "heme-regulated" proteins are still unclear due to the lack of their structural characterizations.

The iron response regulator (Irr) protein in the bacterium *Bradyrhizobium japonicum*, which consists of 163 amino acid residues, is a "heme-regulated" protein and is the global transcriptional regulator of iron homeostasis in that organism (*9*, *10*). Irr binds to the target gene to repress the transcription of the gene's coding enzymes for the heme biosynthesis (*11*), producing quite an interesting regulation mechanism for the transcription. In the presence of iron, Irr degrades to initiate the transcription of the target gene. Such protein degradation by the heme binding to HRM is also found for the regulatory protein in the iron metabolism of the mammalian system (*12*). Therefore, the regulatory function of heme and heme-dependent protein degradation is common in a wide variety of regulatory systems *in vivo*.

Although deletion of the HRM drastically retards the protein degradation of Irr (*11*) and heme binding to the HRM is crucial for the Irr function, the structural information about the heme environments in Irr is still limited. The absorption spectrum for Irr in the presence of the heme is quite unusual in that the Soret peak is highly blue shifted (372 nm) and broad (Figure 1A), suggesting that heme binding to the HRM in Irr is different from those of typical hemoproteins, such as hemoglobin and myoglobin (*11*). Although such a blue-shifted Soret peak has been hypothesized to arise from the ligation of Cys to the heme iron, the cysteine ligation in HRM has not yet been spectroscopically confirmed. Furthermore, the heme stoichiometry for Irr is also unclear. In this study, we determined the heme stoichiometry for

[†]This work was supported by Grants-in-Aid (20051002, K.I.) from the Ministry of Education, Culture, Sports, Science, and Technology in Japan. M.R.O. was supported by National Institutes of Health Grant GM067966.

*Corresponding author. E-mail: koichiro@sci.hokudai.ac.jp. Tel: 81-11-706-2707. Fax: 81-11-706-3501.

[1]Abbreviations: Irr, iron response regulator; HRM, heme-regulatory motif; eNOS, endothelial nitric oxide synthase; CPO, chloroperoxidase; NPAS2, neuronal PAS domain-containing protein 2; Im, imidazole.

 Published on Web 12/30/2010

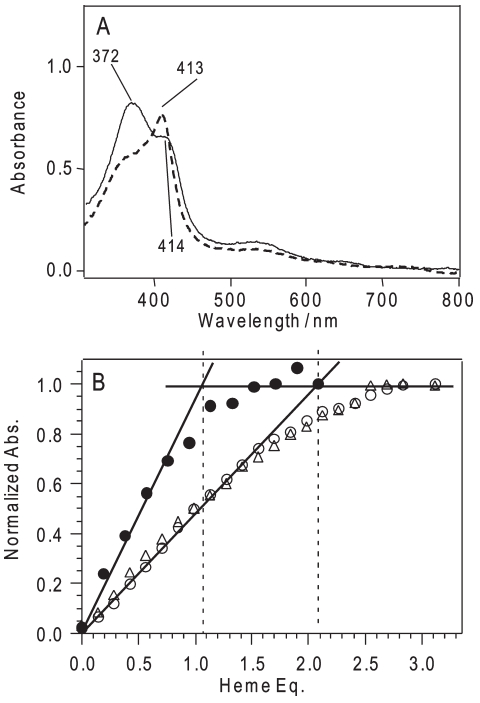

FIGURE 1: Light absorption spectra of heme-bound wild-type Irr and the C29A mutant and heme titration. Panel A: Absorption spectra of heme-bound wild-type Irr (solid line) and the C29A mutant (dashed line). Panel B: Heme titration of wild-type Irr (open symbols) and the C29A mutant (closed symbols). The open and closed circles are the absorbance at 414 nm, and the open triangles are that at 372 nm. The sample concentration is about 10 μM in 50 mM Tris−500 mM NaCl, pH 7.5, at room temperature.

Irr and characterized the coordination structure of heme binding to the HRM in Irr using the absorption, resonance Raman, and EPR spectroscopies, which shed new light on the heme environmental structure in heme-regulated proteins.

MATERIALS AND METHODS

Protein Preparation. The wild-type Irr and ^{29}Cys → Ala (C29A) mutant proteins were expressed in *Escherichia coli* strain BL21(DE3)plysS and purified as described previously (*11*). To prepare heme-bound Irr and its mutant for spectroscopic measurements, we added only a half equivalent of heme (1 mM hemin in a *N*,*N*-dimethylformamide (DMF) solution) to the protein to avoid free hemin in solution, and residual free hemin in solution was removed as much as possible by passing through a PD-10 column (GE Healthcare).

Spectroscopic Heme Titration. Protein and heme concentrations in the solutions for the heme titration were determined using a Perkin-Elmer lambda 19 spectrometer at room temperature. The concentration of Irr was estimated from the extinction coefficient of 18.3 mM^{-1} cm^{-1} at 280 nm (*13*). The heme stock solution was prepared in DMF immediately before use, and the concentration of heme was determined by a pyridine−hemochrome assay (*14*) using the extinction coefficient of 191.5 mM^{-1} cm^{-1} at 418 nm. Spectroscopic titration of the binding of heme to Irr was aerobically performed. A 10 μL heme stock solution (typically 0.3 mM) was repetitively added into the cuvettes containing a solution of 10 μM Irr in 50 mM Tris−500 mM NaCl buffer at pH 7.5 or a solution without Irr at room temperature, and we followed the absorbance difference between the two solutions at 372 and 414 nm.

Resonance Raman Measurements. Resonance Raman spectra were obtained using the system and method reported previously (*15*, *16*). The spectra were obtained by excitation with 363.8 nm light from an argon ion laser (Spectra Physics, BeamLok 2080) (low-frequency region) or 413.1 nm light from a krypton ion laser (Spectra Physics, BeamLok 2060) (high-frequency region). The laser power was ~4 mW for the measurements of heme-bound Irr. The sample concentration was about 50 μM on the heme basis in 50 mM Tris−500 mM NaCl, pH 7.5, at room temperature.

EPR Measurements. The EPR measurements were conducted by the X-band (9.22 GHz) microwave frequency using a Varian E-12 spectrometer with 100 kHz field modulation. The microwave frequency and external magnetic field were calibrated with a Model TR5212 frequency counter (Takeda Riken Co. Ltd.) and a Model EFM 2000AX NMR field meter (ECHO Electronic Co. Ltd.), respectively (*17*). The specific conditions for the measurements are described in the figure legend. An Oxford flow cryostat (ESR-900) was used for measurements at 5 and 15 K. The sample concentration was about 1 mM in 50 mM Tris−500 mM NaCl at pH 7.5. The measurement temperatures were 5 and 15 K to detect the ferric high- and low-spin signals, respectively. The cysteine (Cys) modification by addition of $HgCl_2$ was followed by the procedure reported previously (*18*). The relative concentrations of the low-spin species were quantified by comparing the signal heights of the g_z signals in the EPR spectra at 15 K.

RESULTS AND DISCUSSION

Heme Stoichiometry. To determine the stoichiometry of the heme binding in Irr, we followed the absorbance difference between the solution with and without Irr at 372 and 414 nm. As shown in Figure 1B, the heme titration for the wild-type Irr clearly indicates that it can bind 2 equiv of the heme (open symbol in Figure 1B), as suggested by our previous study (*11*, *19*). To examine heme binding to the sole cysteine residue, ^{29}Cys, in the HRM, we compared the heme stoichiometry of the wild-type and ^{29}Cys-mutated Irr proteins. The spectroscopic heme titration for the C29A mutant was monitored by the Soret band at 414 nm (closed symbol in Figure 1B), showing that the C29A mutant can bind only 1 equiv of the heme, and thus, one heme binding was lost by the mutation at ^{29}Cys. In addition, the Soret band at 372 nm was shifted to 414 nm in C29A (Figure 1A) (*11*, *19*), also supporting the ligation of ^{29}Cys in the HRM to the heme iron in the wild-type Irr.

Fe−S Stretching Mode in Heme-Bound Irr. The absorption spectrum for heme-bound Irr was quite different from that of conventional Cys-ligated proteins, such as P450 and nitric oxide synthase (NOS), with the Soret maximum around 392 nm (Figure 1A) (*11*, *19*), suggesting the unusual heme environmental structure. As the absorption spectrum would not give the detailed structures of the heme binding sites, we measured the resonance Raman spectra to further characterize heme binding to the HRM and other possible heme binding. Figure 2 shows the low-frequency region of the resonance Raman spectra of the heme-bound Irr excited at 363.8 nm, in which the heme iron−cysteine stretching mode is expected to be detected in the region of 310−350 cm^{-1}. To unambiguously assign the Fe−S stretching mode in the heme-bound Irr, we used ^{54}Fe-substituted porphyrin (Figure 2A) and followed the isotopic shift in the resonance Raman spectrum. Despite the rather low signal-to-noise ratio of

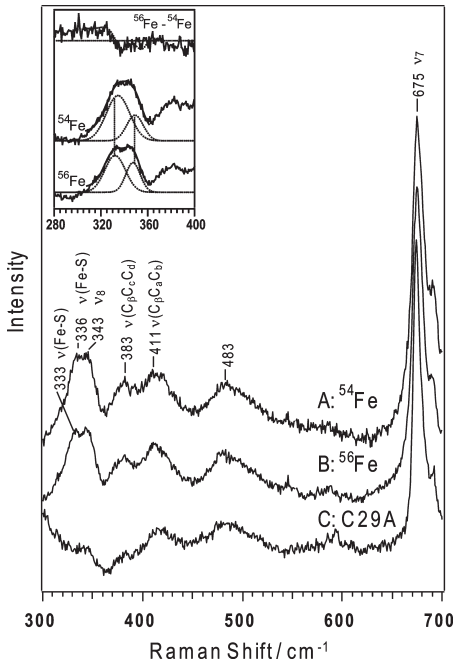

FIGURE 2: Resonance Raman spectra of the low-frequency region for the wild-type ^{54}Fe-heme-bound Irr (A, ^{54}Fe), ^{56}Fe-heme-bound Irr (B, ^{56}Fe), and the ^{56}Fe-heme-bound C29A mutant (C, C29A). The spectra were obtained by excitation with 363.8 nm light from an argon ion laser (Spectra Physics, BeamLok 2080). The inset shows the enlarged Raman line around 340 cm^{-1} for the ^{54}Fe- and ^{56}Fe-heme-bound Irr and their difference spectrum. The Raman lines can be fitted by two Gaussian features (dotted lines) centered at 333 and 343 cm^{-1} for ^{56}Fe-heme-bound Irr and at 336 and 343 cm^{-1} for ^{54}Fe-heme-bound Irr. The solid line is the simulated trace given by the two Gaussian lines.

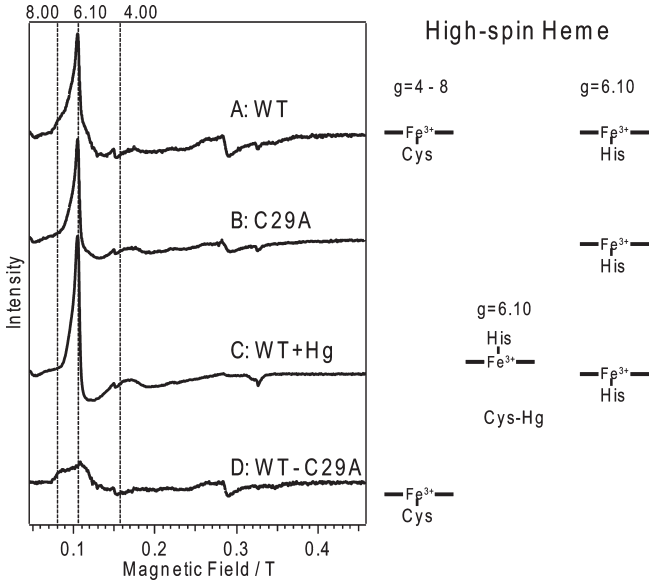

FIGURE 3: EPR spectra of heme-bound Irr (A, WT), the heme-bound C29A mutant (B, C29A), $HgCl_2$-modified heme-bound Irr (C, WT + Hg), and the difference between the heme-bound Irr and C29A (D, WT − C29A (A − B)). The spectra were recorded at 5 K, 10 mW microwave power, 0.5 mT field modulation amplitude. Each EPR spectrum was averaged over four data acquisitions. The *g*-values are labeled on the top of the figure. The schematic coordination structures of the ferric high-spin heme are illustrated on the right-hand side of each EPR spectrum.

the difference spectrum due to irreversible protein aggregation under the laser irradiation, the Raman line at 333 cm^{-1} for the ^{56}Fe-heme-bound Irr clearly showed an isotopic shift (2.5 cm^{-1}) to 336 cm^{-1} for the ^{54}Fe-heme-bound Irr (Figure 2, inset). A positive peak around 325 cm^{-1} and a negative peak around 335 cm^{-1} were reproducible, while other peaks in the difference spectra were not reproducible. The high-frequency region of the resonance Raman spectra of the ^{54}Fe-heme-bound Irr (Figure S1 in Supporting Information) was essentially the same as that of the ^{56}Fe-heme-bound Irr, and thus no significant isotopic shifts were observed for this region.

The isotopic shift (2.5 cm^{-1}) from ^{56}Fe to ^{54}Fe in the Raman line at 333 cm^{-1} in the heme-bound Irr corresponds to that of the Fe−S stretching mode of endothelial nitric oxide synthase (eNOS) (about 2 cm^{-1}) (*20*) and calculated value (*21*), confirming the assignment of the Fe−S stretching mode in Irr. The line at 333 cm^{-1} was not detected in the heme-bound C29A mutant (Figure 2C), also indicating that this line originated from Fe−S (^{29}Cys) stretching in the heme-bound Irr. The Raman line at 343 cm^{-1} in the ^{56}Fe-heme-bound Irr also showed a smaller isotopic shift (1.7 cm^{-1}), suggesting the possibility that the Raman line at 343 cm^{-1} is also assignable to the Fe−S stretching mode, although the ν_8 mode is overlapped on this mode. However, the signal intensity of the Raman line at 343 cm^{-1} is rather weak, compared with that at 333 cm^{-1}; thus the ^{56}Fe-heme-bound Irr with the Fe−S stretching mode at 333 cm^{-1} is predominant.

It should be noted here that the Fe−S stretching frequency, 333 cm^{-1}, of the major fraction of the heme-bound Irr is quite low compared to those of P450cam (351 cm^{-1}) (*21*) and CPO (347 cm^{-1}) (*22*). Thus far, the lowest frequencies of the Fe−S stretching mode in the Cys-ligated hemoproteins were reported for NPAS2 (334 cm^{-1}) (*16*) and eNOS (338 cm^{-1}) (*20*), in which the basicity of the axial thiolate is lower than those in P450 and CPO due to a weakened hydrogen bond between the sulfur atom of the thiolate and the nitrogen atom of the amide group in the main chain. Considering that the frequency of the Fe−S stretching mode of the heme-bound Irr is lower than that of eNOS, ^{29}Cys in the HRM of Irr has no hydrogen bonds with amide groups in the main chain to stabilize the Fe−S bond.

Another characteristic of the Fe−S stretching mode in the heme-bound Irr is the broad line width. The line width of the Fe−S stretching mode is less than 10 cm^{-1} for the typical Cys-ligated hemoproteins (*21*, *22*), while that of the heme-bound Irr is more than 20 cm^{-1}, suggesting that multiple Raman lines from the Fe−S bond overlap. The broad Soret band for the heme-bound Irr also corresponds to multiple configurations of heme binding in Irr. Such a broad Soret band was also reported for the HRM containing heme-regulated proteins such as Hap1 (*23*), Bach1 (*24*), and IRP2 (*12*, *25*). The ligation of ^{29}Cys to the heme iron is, therefore, heterogeneous and distinct from the conventional Cys-ligated hemoproteins, which is characteristic for heme-regulated proteins with the HRM.

Characterization of High-Spin Heme in Heme-Bound Irr. The unusual and multiple configurations of cysteine ligation to the heme in the HRM in Irr are also evident based on the EPR spectrum. Figure 3 shows the EPR spectra at 5 K, where the EPR signals from the high-spin species are clearly observed. While both the EPR spectra of the heme-bound wild-type Irr (Figure 3A) and C29A with heme (Figure 3B) have a sharp signal at $g = 6.10$, the EPR signal in the wild-type Irr (Figure 3A) exhibits broad shoulders around $g = 4$ and $g = 8$, which are completely diminished in the C29A mutant (Figure 3B). Such a broad signal from $g = 4$ to $g = 8$ is more evident in the difference

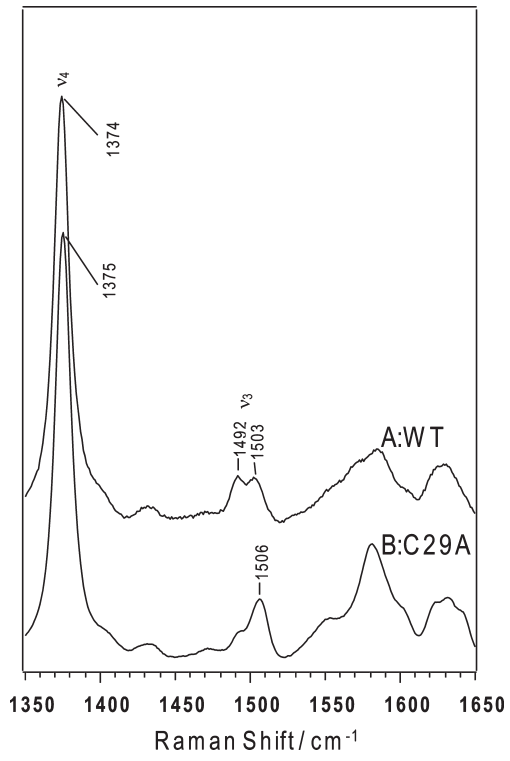

FIGURE 4: Resonance Raman spectra of the high-frequency region of the wild-type heme-bound Irr (A, WT) and the C29A mutant (B, C29A). The spectra were obtained by excitation with 413.1 nm light from a krypton ion laser (Spectra Physics, BeamLok 2060). The laser power was ~4 mW for the measurements of the low- and high-frequency regions. The sample concentration was about 50 μM in 50 mM Tris−500 mM NaCl, pH 7.5, at room temperature.

spectrum (Figure 3D), indicating that the broad signal from $g = 4$ to $g = 8$ is derived from the Cys-ligated heme in the HRM. The broad EPR signal from the Cys-ligated heme is also supported by $HgCl_2$ modification. $HgCl_2$ can specifically react with Cys residues to form the Hg adduct to inhibit the ligation of the heme to Cys (*18*). In the spectrum of the $HgCl_2$-treated heme-bound Irr (Figure 3C), we could not detect broad shoulders around $g = 4$ and $g = 8$, confirming that the broad EPR signal from $g = 4$ to $g = 8$ is derived from the Cys-ligated heme in Irr.

Although previous studies demonstrated the EPR signal from $g = 4$ to $g = 8$ is characteristic of the Cys-ligated 5-coordinate high-spin heme (*26*), the signal pattern is quite different from those of the typical Cys-ligated high-spin hemoproteins (*27*) and model complexes (*28*). Such a broad signal can be the result of the highly overlapped signals derived from the multiple configurations of heme binding to Cys in Irr. The heterogeneous heme binding to ^{29}Cys corresponds to the broad Raman line of the Fe−S stretching mode (Figure 2) as discussed above, which is also distinctly different from those of typical hemoproteins.

The presence of the Cys-ligated 5-coordinate high-spin heme is further supported by the high-frequency region of the resonance Raman spectrum (Figure 4). Two ν_3 lines were observed for the heme-bound Irr (Figure 4A), and the position of one of the lines (1492 cm^{-1}) was close to that of the high-spin component of eNOS (1489 cm^{-1}) (*20*) and typical of the Cys-ligated 5-coordinate high-spin heme (*29*). For C29A, the intensity of the ν_3 line at 1492 cm^{-1} drastically decreased (Figure 4B), indicating that the high-spin species is derived from the ligation of ^{29}Cys to the heme iron.

On the other hand, the commonly observed narrow EPR signal at $g = 6.10$ in the heme-bound wild-type Irr and C29A mutant (Figure 3A,B) can be assignable to the His-ligated high-spin heme. While the intense peak at $g = 6.10$ corresponds to the His-ligated high-spin species in the heme-bound Irr, the light absorption band characteristic of the His-ligated high-spin heme was only observed as a small shoulder peak around 630 nm (Figure 1A), showing that the fraction of the His-ligated high-spin heme is rather small at room temperature. Such an intense high-spin signal in the low-temperature EPR spectrum and the negligible fraction of the high-spin species in the light absorption and resonance Raman spectra at room temperature were also reported in hemoproteins (*25*) and model complexes of hemoproteins (*30*) showing the labile heme binding, corresponding to the multiple configurations in the heme binding of the second heme binding site as found for those of the HRM in Irr.

Although the sharp EPR signal around $g = 6$ was observed for nonspecific heme binding (*25*) and we cannot completely exclude the possibility that Irr can nonspecifically bind hemes on the protein surface, the total amount of the His-ligated high- and low-spin hemes in the heme-bound Irr was almost the same as that of the Cys-ligated heme as discussed in the next section. The second heme binding site remaining in C29A would therefore predominantly have the low-spin heme, and the small fraction of the heme in the second heme binding site might be the His-ligated high-spin species, which increases at low temperature. Thus, we can conclude that heme-bound Irr has the Cys-ligated 5-coordinate high-spin heme with multiple heme binding configurations in the HRM, and the heme in the second heme binding site is predominantly in the low-spin state, where two His residues coordinate with the heme iron. The second heme binding site also shows the labile coordination structure, as found for the HRM.

Characterization of Low-Spin Heme in Heme-Bound Irr. In addition to the high-spin hemes, the heme-bound Irr shows some EPR signals from the low-spin heme. Although the intensities of the low-spin EPR signals were small due to saturation in the measurements at 5 K (Figure 3A), they are less readily saturated and clearly observed in the measurement at 15 K as shown in Figure 5. While the low-spin signals in the heme-bound Irr (Figure 5A) consist of two sets of low-spin signals at $g = (2.52, 2.29, 1.90)$ and $(2.98, 2.29, 1.53)$, the difference EPR spectrum between the wild-type Irr and C29A (Figure 5D), which highlights the coordination structure of ^{29}Cys to the heme iron, shows only one set, $g = (2.52, 2.29, 1.90)$. The addition of $HgCl_2$ to the heme-bound Irr also completely diminished the low-spin component at $g = (2.52, 2.29, 1.90)$ (Figure 5C), resulting in a spectrum similar to that of C29A (Figure 5B). These EPR signals, diminished by the mutation or modification of ^{29}Cys, were also observed for cystathionine β-synthase (*18*) and the imidazole-bound low-spin heme in P450cam (*27*), implying that the heme-bound Irr has a Cys/His-ligated low-spin heme.

To determine the relative fraction of the Cys-ligated low-spin heme to the bound heme in the HRM, we measured the EPR spectrum of the heme-bound Irr in the presence of imidazole. With the addition of 100 mM imidazole (Figure 6B), the intensity of the EPR signals from the low-spin species was enhanced without any shifts in the g-values, compared with that in the heme-bound wild-type Irr (Figure 6A). One of the sets of the low-spin signals, at $g = (2.52, 2.29, 1.90)$, is typical for the Cys/His-ligated heme (*27*), also supporting the ligation of histidine as the axial ligand trans to ^{29}Cys in the absence of imidazole. The addition of imidazole completely converted the high-spin species to a low-spin species with a 4-fold enhancement in the signal

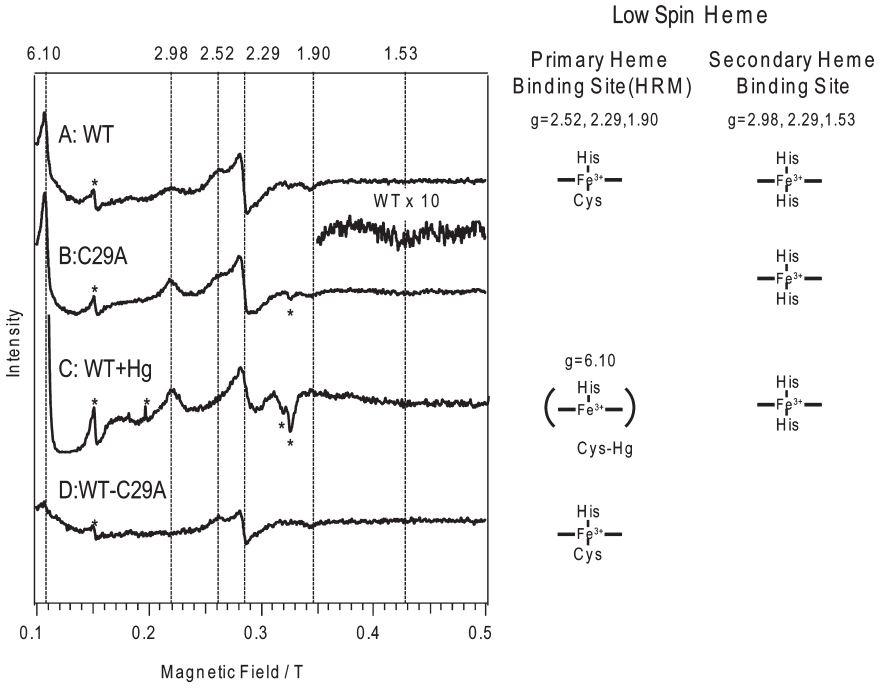

FIGURE 5: EPR spectra of heme-bound Irr (A, WT), the heme-bound C29A mutant (B, C29A), Hg-modified heme-bound Irr (C, WT + Hg), and the difference between the heme-bound Irr and C29A (D, WT − C29A (A − B)). The spectra were recorded at 15 K, 10 mW microwave power, 1 mT modulation amplitude. Each EPR spectrum was averaged over four data acquisitions. The asterisk (*) denotes an artifact signal. The *g*-values are labeled on the top of the figure. The schematic coordination structures of only the ferric low-spin heme species are illustrated on the right-hand side of each EPR spectrum, and the relative concentrations of the low-spin species were quantified by comparing the signal heights of the g_z signals in the EPR spectra.

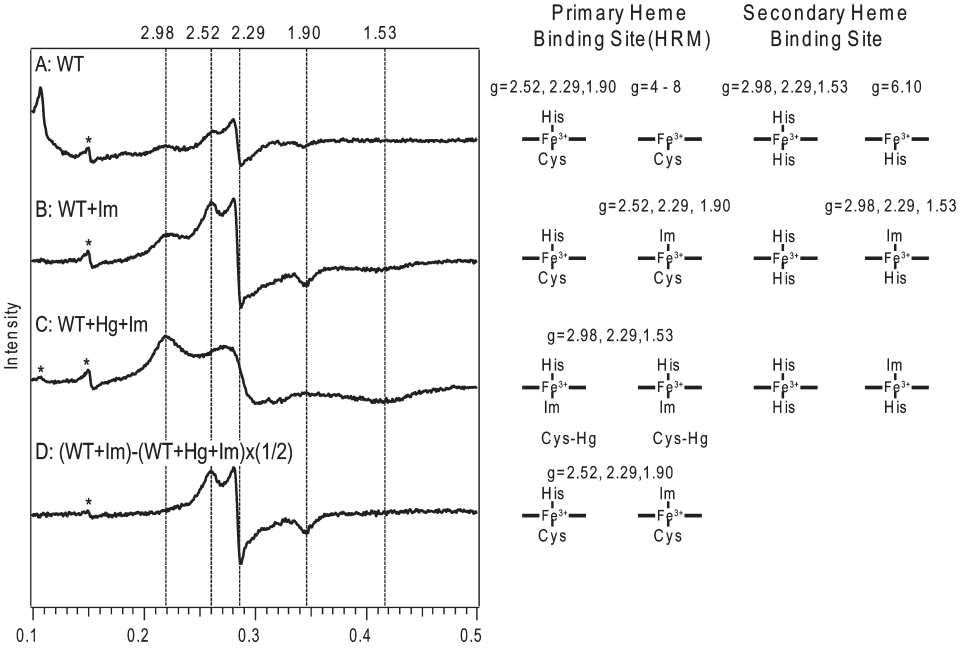

FIGURE 6: EPR spectra of heme-bound Irr (A, WT), the imidazole adduct of heme-bound Irr (B, WT + Im), the imidazole adduct of heme-bound $HgCl_2$-modified Irr (C, WT + Hg + Im), and the difference between the heme-bound Irr and $HgCl_2$-modified Irr in the presence of imidazole (D, (WT + Im) − (WT + Hg + Im) × $^1/_2$ (B − C × $^1/_2$)). The spectra were recorded at 15 K, 10 mW microwave power, 1 mT modulation amplitude. Each EPR spectrum was averaged over four data acquisitions. The asterisk (*) denotes an artifact signal. The *g*-values are labeled on the top of the figure. The coordination structures of the ferric heme species are schematically illustrated on the right-hand side of each EPR spectrum, and the relative concentrations of the low-spin species were quantified by comparing the signal heights of the g_z signals in the EPR spectra.

intensity of the low-spin species at g = (2.52, 2.29, 1.90), implying that the 5-coordinate Cys-ligated species is the major component in the primary heme binding site, HRM.

In addition, the appearance of other low-spin components at g = (2.98, 2.29, 1.53) in the heme-bound Irr (Figure 6A) indicates the presence of His/His-ligated hemes (*31*) in the second heme binding site. The absorption spectrum of the heme-bound C29A mutant also showed a red-shifted Soret band (Figure 1A) (*19*), which is one of the characteristics of low-spin hemoproteins, and in the resonance Raman spectrum for the heme-bound C29A

mutant (Figure 4B), the ν_3 line for the low-spin heme appeared at 1505 cm^{-1} with a small shoulder from the high-spin heme in the low-frequency side, supporting the predominant formation of the low-spin heme in the second heme binding site.

To confirm a 1:1 ratio of the heme binding in the HRM to that in the secondary heme binding site, we measured the EPR spectrum for heme-bound Irr in the presence of $HgCl_2$ and imidazole (Figure 6C). As clearly shown in Figure 6C, addition of $HgCl_2$ and imidazole completely converted the EPR spectrum of the heme-bound Irr into that of the His/His- or His/Im-ligated low-spin heme, with g = (2.98, 2.29, 1.53). If the Irr can bind the heme at the second heme binding site with a comparable affinity to the HRM, then the His/His- or His/Im-ligated heme in the secondary heme binding site would exhibit a similar contribution to the low-spin EPR signals as does the Cys/His-ligated low-spin heme in the HRM. In this case, half of the signal intensity from the His/His- or His/Im-ligated heme would be derived from the second heme binding site in the imidazole adduct of the $HgCl_2$-modified Irr.

We estimated the contribution of the His/His- or His/Im-ligated heme in the second heme binding site to the low-spin EPR signals in the imidazole adduct of the heme-bound Irr (Figure 6B) by subtracting the EPR spectrum for the heme-bound Irr in the presence of $HgCl_2$ and imidazole (Figure 6C) from the heme-bound Irr in the presence imidazole (Figure 6B). If the heme-bound Irr shows 1:1 heme binding between the HRM and secondary heme binding sites and has no nonspecific heme binding at other sites, then the intensity of the EPR signal from the His/His- or His/Im-ligated heme in the second heme binding site in the imidazole adduct of the heme-bound Irr (Figure 6B), where the HRM has the Cys/His- or Cys/Im-ligated heme and the second heme binding site has the His/His- or His/Im-ligated heme, would be half the intensity of the EPR signal from the His/His- or His/Im-ligated heme in the imidazole adduct of the $HgCl_2$-treated heme-bound Irr (Figure 6C), where both of the HRM and the second heme binding sites have the His/His- or His/Im-ligated heme. When we subtracted the EPR spectrum for the heme-bound Irr in the presence of $HgCl_2$ and imidazole with a factor of $^1/_2$ from the heme-bound Irr in the presence of imidazole ((WT + Im) − (WT + Hg + Im) × $^1/_2$, Figure 6D), the contribution from the His/His- or His/Im-ligated heme in the second heme binding site was completely negated and the EPR spectrum, consisting of only the Cys/His-ligated low-spin heme, was obtained. Thus, we can conclude that the 1:1 heme binding between the primary (HRM) and secondary heme binding sites and the His-ligated high-spin heme showing the sharp EPR signal at g = 6.10 is the minor component in the second heme binding site rather than nonspecific heme binding at other sites.

Structural and Functional Significance of Heme Binding in Irr. The structural characterization of heme binding in the HRM of Irr provides new insights into heme binding in heme-regulated proteins. Irr can bind 2 equiv of heme in the primary (HRM) and secondary heme binding sites (Figure 7). In the HRM, ^{29}Cys is the axial ligand for the heme iron, but, unlike typical Cys-ligated hemoproteins, the axial Cys residue (^{29}Cys) in Irr does not form hydrogen bonds with amide groups of the main chain, leading to the labile and multiple configurations in the ligation of Cys to the heme iron. While the Cys-ligated heme is predominantly 5-coordinate high spin, the Cys/His-ligated low-spin heme is formed as the minor component, and the fraction of the Cys/His-ligated low-spin heme increased at low temperature. The heme binding in the second heme binding site is also

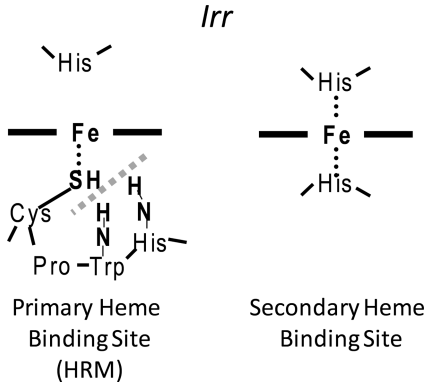

FIGURE 7: Schematic presentation of the heme binding in Irr.

heterogeneous. The major component in the second heme binding site is the low-spin heme, which is coordinated by two His residues we have not yet identified, and a small amount of the His-ligated high-spin heme was also observed.

Such multiple heme binding to heme-regulated proteins has also been reported for Hap1 (*6*, *32*) and Bach1 (*24*), and all of the hemes bound for these proteins have been supposed to be ligated to Cys residues in the HRM, although the detailed analysis for the heme binding in these heme-regulated proteins has not yet been done. On the other hand, Irr has only one HRM in the sequence, but it can bind 2 equiv of heme, and one of the heme binding sites, which shows the His/His ligation, is outside the HRM. Although we have not yet identified the His residues coordinating with the heme in the secondary heme binding site and the functional significance of the His/His-ligated heme binding is still unclear, the heme binding outside the HRM region in Irr shows the possibility that the other heme-regulated proteins also can bind the heme outside of the HRM region, and careful reconsideration might be required for heme binding in heme-regulated proteins.

Another characteristic of heme binding in Irr is the multiple configurations of the heme binding, which is definitely different from the typical Cys-ligated hemoproteins. As evident by the highly specific enzymatic reactions of conventional hemoproteins, the heme environmental structures of these hemoproteins are rationally designed and regulated for their functions, which require highly homologous structures of the heme active center. On the other hand, the heme in Irr is not the active center for the enzymatic reaction as found for the conventional functions in hemoproteins but the trigger for oxidative modification and protein degradation. The essential function of heme in Irr is supposed to be the generation of reactive oxygen species (ROS) for the oxidative modification of the protein, where high specificity would not be required (*33*). The ligation of the heme to the simple consensus sequence of HRM, Cys and Pro, resulted in heterogeneous and multiple configurations in heme binding, which would not be sufficient for highly specific and catalytic oxidation of the substrates as found for heme peroxidases and oxygenases but enough to generate ROS for oxidative modification for protein degradation. The function of the heme in Irr is, therefore, quite different from those of the conventional hemoproteins, leading to multiple configurations in heme binding.

In summary, on the basis of the EPR and resonance Raman spectra, we confirmed heme binding to ^{29}Cys in the HRM and found another heme binding in the secondary heme binding site, in which two His residues can be ligated to the heme in Irr. We also structurally characterized these heme binding sites and

revealed the weak heme axial bond and multiple configurations in the primary heme binding site, HRM, showing that the heme environment of the HRM in Irr is quite different from that in typical Cys-ligated hemoproteins. In the second heme binding site, the coordination of His is also rather labile, compared with that in other hemoproteins, and shows temperature-dependent dissociation of the axial ligand. Such unusual heme binding is characteristic of heme-regulated proteins having HRM as the heme binding site.

ACKNOWLEDGMENT

We are grateful of Prof. T. Kitagawa (Okazaki Institute for Integrative Bioscience) for kind permission to use his resonance Raman observating system.

SUPPORTING INFORMATION AVAILABLE

Details of experimental procedures. This material is available free of charge via the Internet at http://pubs.acs.org.

REFERENCES

1. Ponka, P. (1999) Cell biology of heme. *Am. J. Med. Sci. 318*, 241–256.
2. Kaasik, K., and Lee, C.C. (2004) Reciprocal regulation of haem biosynthesis and the circadian clock in mammals. *Nature 430*, 467–471.
3. Yin, L., Wu, N., Curtin, J. C., Qatanani, M., Szwergold, N. R., Reid, R. A., Waitt, G. M., Parks, D. J., Pearce, K. H., Wisely, G. B., and Lazar, M. A. (2007) Rev-erbα, a heme sensor that coordinates metabolic and circadian pathways. *Science 318*, 1786–1789.
4. Faller, M., Matsunaga, M., Yin, S., Loo, J. A., and Guo, F. (2007) Heme is involved in microRNA processing. *Nat. Struct. Mol. Biol. 14*, 23–29.
5. Chen, J.-J., and London, I. M. (1995) Regulation of protein synthesis by heme-regulated eIF-2α kinase. *Trends Biochem. Sci. 20*, 105–108.
6. Zhang, L., and Guarente, L. (1995) Heme binds to a short sequence that serves a regulatory function in diverse proteins. *EMBO J. 14*, 313–320.
7. McCoubrey, W. K., Huang, T. J., and Maines, M. D. (1997) Heme oxygenase-2 is a hemoprotein and binds heme through heme regulatory motifs that are not involved in heme catalysis. *J. Biol. Chem. 272*, 12568–12574.
8. Yang, J., Kim, K. D., Lucas, A., Drahos, K. E., Santos, C. S., Mury, S. P., Capelluto, D. G. S., and Finkielstein, C. V. (2008) A novel heme-regulatory motif mediates heme-dependent degradation of the circadian factor period 2. *Mol. Cell. Biol. 28*, 4697–4711.
9. Yang, J., Sangwan, I., Lindemann, A., Hauser, F., Hennecke, H., Fischer, H.-M., and O'Brian, M. R. (2006) *Bradyrhizobium japonicum* senses iron through the status of haem to regulate iron homeostasis and metabolism. *Mol. Microbiol. 60*, 427–437.
10. Hamza, I., Chauhan, S., Hassett, R., and O'Brian, M. R. (1998) The bacterial Irr protein is required for coordination of heme biosynthesis with iron availavility. *J. Biol. Chem. 273*, 21669–21674.
11. Qi, Z., Hamza, I., and O'Brian, M. R. (1999) Heme is an effector molecule for iron-dependent degradation of the bacterial iron response regulator (Irr) protein. *Proc. Natl. Acad. Sci. U.S.A. 96*, 13056–13061.
12. Ishikawa, H., Kato, M., Hori, H., Ishimori, K., Kirisako, T., Tokunaga, F., and Iwai, K. (2005) Involvement of heme regulatory motif in heme-mediated ubiquitination and degradation of IRP2. *Mol. Cell 19*, 171–181.
13. Gill, S. C., and von Hippel, P. H. (1989) Calculation of protein extinction coefficients from amino acid sequence data. *Anal. Biochem. 182*, 319–326.
14. Berry, E. A., and Trumpower, B. L. (1987) Simultaneous determination of hemes *a*, *b*, and *c* from pyridine hemochrome spectra. *Anal. Biochem. 161*, 1–15.
15. Ishikawa, H., Yun, B.-G., Takahashi, S., Hori, H., Matts, R. L., Ishimori, K., and Morishima, I. (2002) NO-induced activation mechanism of the heme-regulated eIF2α kinase. *J. Am. Chem. Soc. 124*, 13696–13697.
16. Uchida, T., Sato, E., Sato, A., Sagami, I., Shimizu, T., and Kitagawa, T. (2005) CO-dependent activity-controlling mechanism of heme-containing CO-sensor protein, neuronal PAS domain protein 2. *J. Biol. Chem. 280*, 21358–21368.
17. Inuzuka, T., Yun, B.-G., Ishikawa, H., Takahashi, S., Hori, H., Matts, R. L., Ishimori, K., and Morishima, I. (2004) Identification of crucial histidines for heme binding in the N-terminal domain of the heme-regulated eIF2α kinase. *J. Biol. Chem. 279*, 6778–6782.
18. Ojha, S., Hwang, J., Kabil, O., Penner-Hahn, J. E., and Banerjee, R. (2000) Characterization of the heme in human cystathionine β-synthase by X-ray absorption and electron paramagnetic resonance spectroscopies. *Biochemistry 39*, 10542–10547.
19. Yang, J., Ishimori, K., and O'Brian, M. R. (2005) Two heme binding sites are involved in the regulated degradation of the bacterial iron response regulator (Irr) protein. *J. Biol. Chem. 280*, 7671–7676.
20. Schelvis, J. P. M., Berka, V., Babcock, G. T., and Tsai, A.-l. (2002) Resonance Raman detection of the Fe-S bond in endothelial nitric oxide synthase. *Biochemistry 41*, 5695–5701.
21. Champion, P. M., Stallard, B. R., Wagner, G. C., and Gunsalus, I. C. (1982) Resonance Raman detection of an iron-sulfur bond in cytochrome P 450cam. *J. Am. Chem. Soc. 104*, 5469–5472.
22. Bangcharoenpaurpong, O., Champion, P. M., Hall, K. S., and Hager, L. P. (1986) Resonance Raman studies of isotopically labeled chloroperoxidase. *Biochemistry 25*, 2374–2378.
23. Hon, T., Hach, A., Tamalis, D., Zhu, Y., and Zhang, L. (1999) The yeast heme-responsive transcriptional activator Hap1 is a preexisting dimer in the absence of heme. *J. Biol. Chem. 274*, 22770–22774.
24. Hira, S., Tomita, T., Matsui, T., Igarashi, K., and Ikeda-Saito, M. (2007) Bach1, a heme-dependent transcription factor, reveals presence of multiple heme binding sites with distinct coordination structure. *IUBMB Life 59*, 542–551.
25. Dycke, C., Bougault, C., Gaillard, J., Andrieu, J.-P., Pantopoulos, K., and Moulis, J.-M. (2007) Human iron regulatory protein 2 is easily cleaved in its specific domain: consequences for the haem binding properties of the protein. *Biochem. J. 408*, 429–439.
26. Sakurai, H., Hatayama, E., Yoshimura, T., Maeda, M., Tamura, H., and Kawasaki, K. (1983) Thiol-containing peptide-hemin complexes as models of cytochrome P-450. *Biochem. Biophys. Res. Commun. 115*, 590–597.
27. Dawson, J. H., Andersson, L. A., and Sono, M. (1982) Spectroscopic investigations of ferric cytochrome P-450-CAM ligand complexes. Identification of the ligand trans to cysteinate in the native enzyme. *J. Biol. Chem. 257*, 3606–3617.
28. Wells, A. V., Li, P., Champion, P. M., Martinis, S. A., and Sligar, S. G. (1992) Resonance Raman investigation of *Escherichia coli*-expressed *Pseudomonas putida* cytochrome P450 and P420. *Biochemistry 31*, 4384–4393.
29. Spiro, T. G., and Li, X.-Y. (1988) Biological Applications of Raman Spectroscopy (Spiro, T. G., Ed.) pp 1−37, John Wiley & Sons, New York.
30. Nastri, F., Lombardi, A., Morelli, G., Pedone, C., Pavone, V., Chottard, G., Battioni, P., and Mansuy, D. (1998) Hemoprotein models based on a covalent helix-heme-helix sandwich. 3. Coordination properties, reactivity and catalytic application of Fe(III)- and Fe(II)-mimochrome I. *J. Biol. Inorg. Chem. 3*, 671–681.
31. Loew, G. M. H. (1970) An analysis of the electron spin resonance of low spin ferric heme compounds. *Biophys. J. 10*, 196–212.
32. Hon, T., Hach, A., Lee, H. C., Chen, T., and Zhang, L. (2000) Functional analysis of heme regulatory elements of the transcriptional activator Hap1. *Biochem. Biophys. Res. Commun. 273*, 584–591.
33. Yang, J., Panek, H. R., and O'Brian, M. R. (2006) Oxidative stress promotes degradation of the Irr protein to regulate haem biosynthesis in *Bradyrhizobium japonicum*. *Mol. Microbiol. 60*, 209–218.